A neural network-based ECMS for optimized energy management of plug-in hybrid electric vehicles

A Neural Network-based ECMS for Optimized Energy Management of Plug-in Hybrid Electric Vehicles

Zhihang Chen[1], Yonggang Liu[1*], Yuanjian Zhang[2], Zhenzhen Lei[3], Zheng Chen[4, 5*] and Guang Li[5]
[1]State Key Laboratory of Mechanical Transmissions & College of Mechanical and Vehicle Engineering, Chongqing University, Chongqing, 400044, China
[2]Sir William Wright Technology Center, Queen's University Belfast, Belfast, BT9 5BS, United Kingdom
[3]School of Mechanical and Power Engineering, Chongqing University of Science & Technology, Chongqing, 401331, China
[4]Faculty of Transportation Engineering, Kunming University of Science and Technology, Kunming, 650500, China
[5]School of Engineering and Materials Science, Queen Mary University of London, London, E1 4NS, UK
Correspondence: andylyg@umich.edu (Y. Liu) and chen@kust.edu.cn (Z. Chen)

Abstract: For plug-in hybrid electric vehicles, the equivalent consumption minimum strategy is typically regarded as a battery state of charge reference tracking method. Thus, the corresponding control performance is strongly dependent on the quality of state of charge reference generation. This paper proposes an intelligent equivalent consumption minimum strategy based on dual neural networks and a novel equivalent factor correction, which can adaptively regulate the equivalent factor to achieve the near-optimal fuel economy without the support of the state of charge reference. The Bayesian regularization neural network is constructed to predict the near-optimal equivalent factor online, while the backpropagation neural network is designed to forecast the engine on/off with the aim of improving the quality of equivalent factor prediction. The corresponding neural network training takes advantage of the global optimality of dynamic programming. Besides, the novel equivalent factor correction can guarantee that the electrical energy is gradually consumed along the trip and the terminal battery state of charge satisfies the preset constraints. A series of virtual simulations under a total of nine driving cycles demonstrates that the proposed method can deliver a competitive fuel economy comparing to the optimal solution derived from the dynamic programming, as well as regulating the battery state of charge to reach the desired terminal value at the end of the trip.

Key Words: Plug-in Hybrid Electric Vehicles, Bayesian Regularization Neural Network, Intelligent Equivalent Consumption Minimum Strategy, Equivalent Factor Online Correction.

I. INTRODUCTION

Widely accepted, the electrified powertrain system is the most promising technology for addressing the air pollution and energy crisis in transportation sector. Thanks to invertible energy storage devices and electric motors,

the electrification enables vehicles to recover baking energy and introduces an additional degree of freedom for the power-flow distribution control, potentially enhancing overall powertrain efficiency and fuel economy. Thus, numerous efforts have been devoted to developing electrified powertrain configurations and corresponding control strategies. In particular, the popularity of plug-in hybrid electric vehicles (PHEVs) are increasing in both the automotive industry and academia [1]. For PHEVs, the vehicle's energy storage system can be not only charged by the engine-driven generator but the external electric power source. Thus, compared with conventional hybrid electric vehicles (HEVs), a larger capacity battery is normally mounted in PHEVs to store cheaper electrical energy from external sources, which has the great potential of improving the fuel economy [2]. Moreover, the large-capacity battery allows the integration of one or multiple powerful traction motors in the electrified propulsion system, which can restrain the internal combustion engine (ICE) from operating in low-toque and low-efficiency regions. Additionally, PHEVs with the large-capacity battery is able to prolong the endurance mileage, thereby alleviating the range anxiety to a certain extent [3].

Due to the existence of multiple power sources in the electrified powertrain system, the resulting flexibility and complexity of the energy flow require a sophisticated energy management strategy (EMS) to distribute the power demand optimally among all onboard power sources. Generally speaking, EMSs can be categorized as rule-based, optimization-based, and learning-based strategies. Rule-based EMSs are beneficial from the straightforward structure, low computational cost, and ease of implementation, thereby becoming the common choice for commercial hybrid vehicles [4]. Nevertheless, the inherent rigidity of rule-based EMSs is the inevitable defect that causes the low adaptiveness to the dynamic and complex real-world driving conditions. Hence, rule-based EMSs consistently have difficulties finding optimal management solutions in practice [5]. On the contrary, optimization-based EMSs intend to pursue optimal energy consumption by minimizing a fuel-related cost function and, therefore, maximize the benefits of powertrain hybridization. Dynamic programming (DP) is the most preferred global optimization algorithm to solve the energy management problem for hybrid vehicles [6], thanks to its distinguished capability to solve constrained and nonlinear optimization problems. Whereas, due to the serve computational burden and strong dependence on the prior knowledge of future driving conditions, the DP method is inapplicable for the real-time energy management system. It is typically regarded as a benchmark to explore the maximum fuel

economy improvement, thereby evaluating performance or extracting the optimal control parameters for alternative EMSs [7]. Instantaneous optimization algorithms, compared with global ones, can obtain a trade-off between the computational cost and fuel economy optimality. Essentially, the fuel-related cost function is optimized instantaneously without gathering comprehensive information of entire driving conditions in advance. The resulting local-optimal power flow distribution can offer fuel economy close to that of global optimization methods [8]. Learning-based EMSs have been rapidly developed thanks to the recent advances in machine learning and artificial intelligence techniques for data-based network training approaches [9]. The excellent generalization and prediction capabilities of learning methods enable EMSs to learn from the globally optimized control actions and, afterwards, apply them locally. Reinforcement learning and neural network learning are standard leaning methods in terms of the EMSs' design.

Among the existing EMSs, the equivalent consumption minimum strategy (ECMS), a representative of instantaneous optimization algorithms, is the most promising online EMSs and has been widely used in practical applications at present [10, 11]. This method, derived from the Pontryagin's minimum principle (PMP), was initially proposed for HEVs by Paganelli [12]. The basic concept of ECMSs is to unify the ICE fuel consumption and the battery electrical energy consumption into a single variable representing the fuel economy of vehicles. The single variable is referred to as equivalent fuel consumption. The unification as mentioned above enables the feasibility of the instantaneous optimization of the total energy consumption, including both fuel and electrical energy. The fuel-electricity conversion process is performed by introducing an equivalent factor (EF) that weighs the electrical energy expenditure as an equivalent quantity of fuel consumption. For the sake of pursuing maximum energy saving, the EF should be a volatile value and tunned dynamically on the basis of powertrain operations in real time. Consequently, a variety of EF estimation methods have been proposed to adaptively regulate EF considering the vehicle status and driving conditions. Regarding HEVs' applications, it is expected that the EF is regulated according to the parameters related to the battery state of charge (SOC) at each instant, aiming to suppress the excessive SOC deviation from the desired constant. For example, a tangent-shape function of the SOC deviation was employed to correct the EF, to ensure the vehicle charge-sustaining [13]. Unsimilar to HEVs, PHEVs attempts to fully deplete the battery power at the end of the current trip and recharged before the next trip. Thus, the desired

SOC trajectory for PHEVs is no longer a constant. Ideally, SOC should decline gradually along with the travel distance to reach the admissible minimum at the end of the trip. In other words, a SOC reference trajectory is required for PHEVs to guide power flow distribution along the trip, thereby ensuring both optimal energy consumption and the desired value of the terminal SOC. For simplicity, some researchers proposed to define the SOC reference trajectory as a linear function of the remaining trip distance, while only delivering the sub-optimal fuel economy [14-16]. The SOC reference trajectory planning can be improved by introducing the extra variables on top of the trip distance, such as future average speed [17] or predicted power demand [18]. Besides, artificial neural networks (NNs), such as recurrent NN (RNN) [19] and neuro-fuzzy system [20], also can be applied to generate the SOC reference trajectory based on the historical driving data. The NN-enhanced SOC reference generator takes advantage of the outstanding learning ability of NN, which facilitates full use of implicit knowledge from optimal SOC reference trajectories of different driving cycles. Given the existence of the SOC reference trajectory, the EF online regulation can be simplified as the SOC tracking problem. In other words, the tracking methods, such as PID controllers [21, 22] and map-based methods [1], have to be employed to adjust the EF with the aim of tracking SOC reference. It should be noted that both the inevitable imperfections of SOC reference generation and SOC tracking errors contribute to control performance degradation. To eliminate the twofold defects causing sub-optimal performance, EF online estimation method should regulate the EF intelligently without the support of the SOC reference trajectory, as well as guaranteeing not only SOC ending at the desired value but the optimal fuel economy. This ideal scenario is achievable by applying the data-driven NN-enhanced ECMS. Xie et al. [3] constructed a common three-layer backpropagation NN to predict the EF online with three accessible input variables, including the current power demand, the battery SOC, and the ratio of the travelled distance to the total distance. The training simples were extracted from the global optimal solutions over 4 real-world bus driving cycles. Without the SOC reference, the network verification over test driving cycle shows that the SOC is able to terminate at the desired value within an accepted toleration. Moreover, merely around 1.5% fuel economy deterioration can be expected when comparing the proposed NN-enhanced ECMS with the global optimized offline controller. However, the weakness of Xie's research is the lack of robustness test for the proposed method, as there is only one driving cycle selected for the network verification. Even worse, only city bus routes, which are quite regular and

similar, were selected for both network training and verification. Note that only few researches, to the authors' knowledge, have been conducted to investigate intelligent ECMS for PHEVs' energy management without the SOC reference trajectory.

In conclusion, the SOC reference generator is typically employed in EMSs for PHEVs, thereby ensuring that the electrical energy is gradually and optimally depleted along the trip. Concerning ECMS applications, EF regulation methods are primarily conceived to track the given SOC trajectory. Nevertheless, both SOC reference generation and tracking unavoidably result in the control performance degradation due to their parasitic deficiencies, such as sub-optimal SOC trajectory generation and tracking errors. To remove the aforementioned twofold deficiencies, an NN-enhanced ECMS is herein developed in this research, which consists of ECMS as the core algorithm and two NNs to regulate the EF online. One NN is trained to directly predict the EF, while the other is to recognize the optimal engine on/off status with the aim of correcting the predicted EF. In this manner, the EF is adaptively and optimally regulated by the combined NNs based on the influential driving features. Regarding the NN training, the training dataset with inputs and outputs is extracted from optimized control actions over selected driving cycles. The global optimization is achieved by the DP algorithm with the objective to minimize the total equivalent fuel consumption over the entire driving cycle. Moreover, the SOC-distance factor is proposed to further correct the predicted EF for the purpose of reaching the desired terminal SOC. Last, the proposed NN-based ECMS is validated over two test driving cycles to demonstrate its adaptiveness to different driving conditions and the optimality of power distribution management. The main contributions of this research can be summarized into the following three aspects: (1) the Bayesian regularized NN (BRNN) is, to the authors' knowledge, first proposed to predict the EF for ECMS online application. Compared with Levenberg–Marquardt training algorithm, the main merit of the Bayesian regularization is the capability of developing considerable generalized quality networks [23]. The resulting accuracy and prediction performance are justified in this research; (2) a classification NN is utilized to predict the engine on/off status, so as to adjust the predicted EF to lessen the side effects of the prediction error; (3) a novel EF correction factor is introduced to ensure that the terminal SOC reaches at the desired value at the end of the trip. Thus, the SOC reference trajectory generation is excluded in the energy management system, thereby eliminating its parasitic deficiencies.

The remainder of this paper is organized as follows. Section II describes the PHEV powertrain model for EMS performance evaluation. Section III demonstrates the overall structure of the proposed NN-based ECMS firstly. The basic ECMS and DP optimization procedure is then presented, followed by detailing the data processing method for the training data preparation. Afterwards, the novel EF correction method is discussed. The NN quality assessment is presented at the end of this section. Section VI displays important results in terms of the fuel economy. Finally, the main conclusions are summarized in Section V.

II. PHEV Powertrain Modeling

In this study, a power-split PHEV is selected for NN-Based ECMS tuning, testing, and validation. The powertrain system consists of a 39 ampere-hour (Ah) Lithium-ion battery, two electric motors (Motor 1 and Motor 2), a planetary gear set, and a 2-L gasoline engine, as illustrated in Fig. 1. The engine, Motor 1, and Motor 2 connect with the planet carrier, the ring gear, and the sun gear, respectively. Since the dynamic characteristic is often neglected for ease of EMS design, the fuel map of ICE is inserted to characterize the engine performance. Motor 1 can operate as either a traction motor or a generator, while Motor 2 is employed mainly to provide propulsion power. The main specifications of the powertrain system are summarized in Table I.

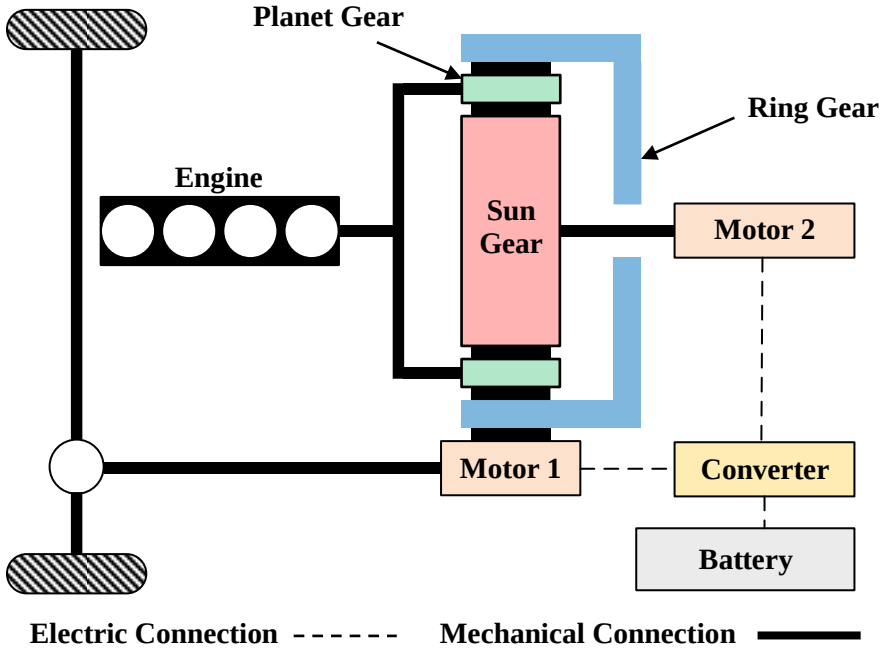

Fig. 1. Power-split PHEV powertrain structure

Table I. Main parameters of power-split PHEV

Parts	Parameters	Value
Vehicle	Total Mass	1801 kg
Battery	Rated Capacity	47.03 Ah
	Rated Voltage	233.89 V
Motor 1/2	Peak Power	70 kW/50 kW
Engine	Cylinder No.	4
Planetary Gear Set	Ring Gear Teeth	83
	Sun Gear Teeth	37
Final Drive Ratio	Gear Ratio	3.02

Given simplification, effectiveness and modelling accuracy of the battery simulation, the internal resistance battery (R_{int}) model is utilized to characterize the electrical performance of the battery in this research. Besides, only the vehicle longitudinal motion is considered as the road load. In other words, the steering dynamic and lateral dynamics are neglected in this research. Additionally, the road topography is assumed flat for all investigations.

III. Structure and Design Process of NN-based ECMS

Due to the prominent performance in balancing between global optimization and real-time implementation, ECMS is employed as the core algorithm of energy management in this paper. Aiming to improve the adaptiveness of ECMS to the uncertainties of the real-world driving conditions, the NN-based EF estimation method is proposed to learn from the optimized control actions under selected driving cycles. Note that the EF prediction error may result in operating the engine to provide the propulsion power when the optimal control decision is to utilize the electric power solely. To avoid such incidents, an extra NN is trained to predict the engine status, which enables the proposed method to decrease the value of the predicted EF at engine-off scenario and, therefore, consolidates the engine shutdown event. The downscaling factor of 0.95 is selected to reduce the EF in this scenario. The design process of the NN-enhanced ECMS can be divided into the offline design part and online implementation part.

The offline design consists of three steps. The first step is the training dataset generation, carrying out by DP global optimization method. The optimization objective is to minimize fuel consumption globally by optimizing EF trajectories over designated driving cycles. Subsequently, driving feature selection is inspired by the relevant researches and regarded as the inputs of the proposed NNs. Principal component analysis (PCA) is introduced to

reduce the dimensionality of the dataset, while remaining significant features that are enough to describe the problem with sufficient accuracy. The third step is the offline training of two NNs concerning the engine on/off status and the optimal EF, respectively.

In terms of the online part, the proposed energy management control strategy comprises four modules: ECMS as the core control algorithm, a well-trained BRNN as the EF predictor, a classification NN as the EF modification for engine-off scenario, and the EF correction for the terminal SOC restraint. Note that for the online implementation of the proposed EMS, the destination of the upcoming trip is required to be known in prior. Besides, it is assumed that the historical travel information can be accumulated to calculate the travelled distance instantaneously. Both two assumptions can be easily realized in practice with the assistance of the global position system (GPS) and geographic information system (GIS). The sketch of the design process and detailed NN-based ECMS architecture are summarized in Fig. 3.

The following subsections present the details of the offline design process for EF BRNN predictor and engine status NN classifier. First, the basic ECMS is demonstrated with the EF global optimization method. Second, driving cycles are selected and constructed for DP optimization to obtain globally optimal solutions for NN training. Then, the optimal solutions are processed and re-constructed to establish the training dataset. Later, the EF correction method is elaborated, followed by the description of the structures of both EF BRNN predictor and engine status NN classifier. Final, the quality of trained NNs is assessed by comparing NN outputs and targets.

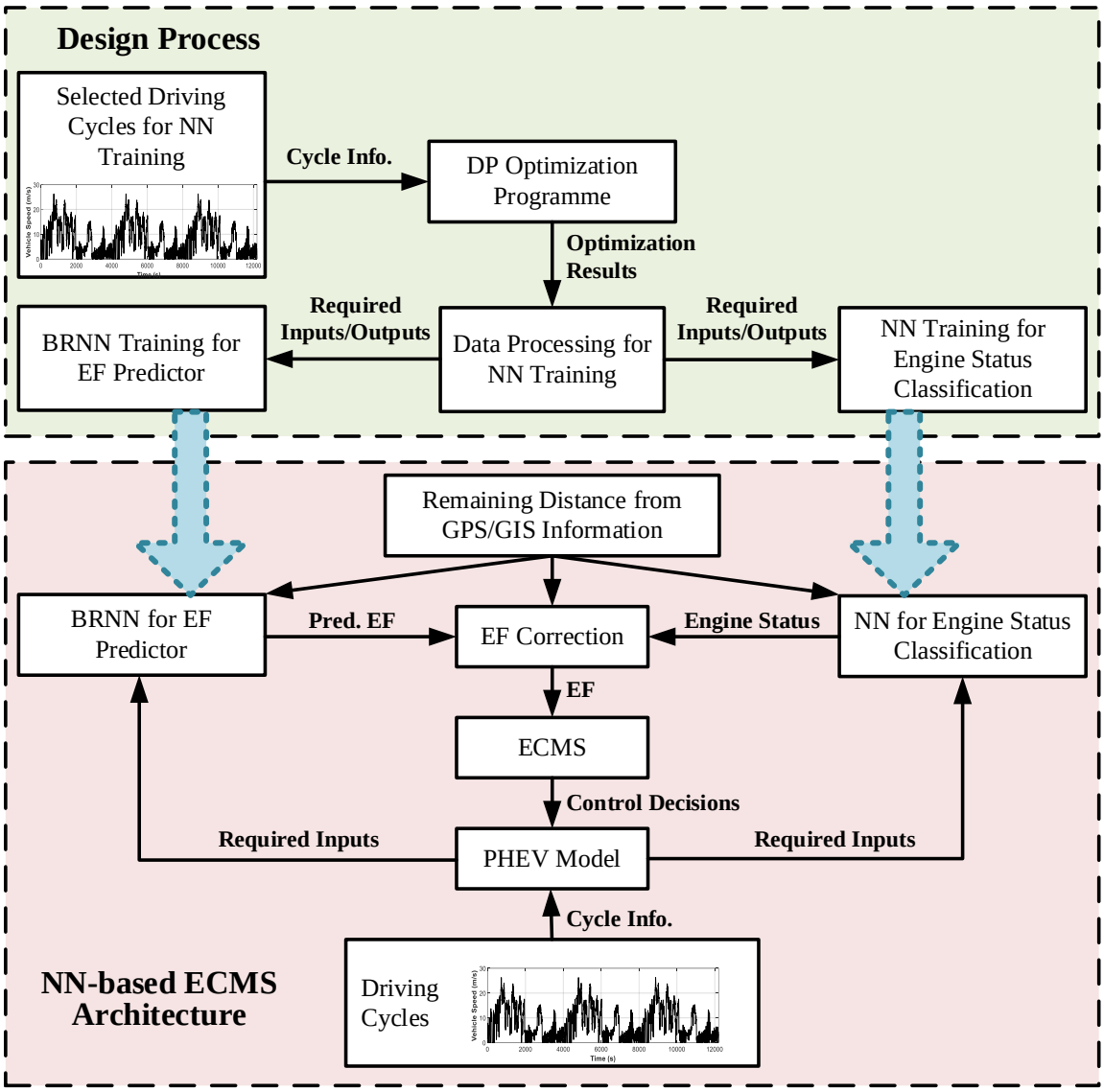

Fig. 2. Design process (upper block) and structure of the proposed NN-based ECMS

A. ECMS and EF optimization method

For a given driving cycle, solving the optimal control problem is to find the optimal control sequence within admissible control limits by minimizing the fuel-related cost function. In this research, the cost function can be mathematically summarized as,

$$J = \phi_f(x(t_f)) + \int_{t_0}^{t_f} \dot{m}_f(x(t), u(t))dt \quad (1)$$

where J is integral performance index. $\phi_f(x(t_f))$ represents all prescribed constraints on the final state. $x(t)$ represents the state variable. t_0 and t_f is the beginning and ending time of the trip. $\dot{m}_f$ is the fuel flow rate. $u(t)$ represents the control variables which could be engine output torque, battery power, etc.

The battery SOC is chosen as the state variable $x(t)$, and the control variables $u(t)$ is the EF $\lambda(t)$,

$$x(t) = SOC(t) \tag{2}$$

$$u(t) = \lambda(t) \tag{3}$$

Based on the concept of ECMS, the optimal control at each instant is achieved by selecting the optimal power distribution that instantaneously minimizes total equivalent fuel consumption. Thus, derived from Eq. (7), the objective function in ECMS is expressed as,

$$J = \int_{t_0}^{t_f} \dot{m}_{equ}(x,u,t)dt \tag{4}$$

Subject to the physical constraints on the power components as follows,

$$\begin{cases} P_{eng\_\min} \le P_{eng} \le P_{eng\_\max}, \omega_{eng\_\min} \le \omega_{eng} \le \omega_{eng\_\max}, T_{eng\_\min} \le T_{eng} \le T_{eng\_\max} \\ P_{mot1\_\min} \le P_{mot1} \le P_{mot1\_\max}, \omega_{mot1\_\min} \le \omega_{mot1} \le \omega_{mot1\_\max}, T_{mot1\_\min} \le T_{mot1} \le T_{mot1\_\max} \\ P_{mot2\_\min} \le P_{mot2} \le P_{mot2\_\max}, \omega_{mot2\_\min} \le \omega_{mot2} \le \omega_{mot2\_\max}, T_{mot2\_\min} \le T_{mot2} \le T_{mot2\_\max} \\ P_{bat\_\min} \le P_{bat} \le P_{bat\_\max}, SOC_{\min} \le SOC \le SOC_{\max} \end{cases} \tag{5}$$

where T and ω denote torque and speed, respectively. The subscript eng, $mot1$ and $mot2$ mean the engine, Motor 1 and Motor 2, respectively. The indexes $\min$ and $\max$ represent the upper and lower boundaries. $\dot{m}_{equ}$ is the instantaneous equivalent fuel consumption, which is the sum of battery equivalent consumption $\dot{m}_{ele}$ and the actual fuel consumption $\dot{m}_{eng}$ at each instant, expressed as,

$$\dot{m}_{equ} = \dot{m}_{eng} + \dot{m}_{ele} \tag{6}$$

Battery equivalent fuel consumption can be calculated as,

$$\dot{m}_{ele}(t) = \lambda(t)\frac{P_{bat}}{LHV} \tag{7}$$

where LHV represents the fuel lower heating value.

In this research, the optimal EF trajectory is obtained offline by means of DP algorithm for given driving cycles, and regarded as the training dataset for the EF NN-based estimation model. DP algorithm can decompose a multistage control problem into a sequence of interrelated one-stage problems that can be solved recursively [24]. In each sub-problem, the control and state variables are discretized. The costs of all admissible control actions can be evaluated by the prescribed cost function over all state and control grids exhaustively, and memorized in a matrix of costs. Subsequently, DP algorithm finds the optimal sequence control actions that minimize the cost function globally while satisfying all constraints. Note that DP proceeds the cost evaluation backward, this is, in this research the equivalent fuel consumption from step $(N-1)$ to the last step N is calculated first. The cost-to-go function for step $(N-1)$ is

$$J_{N-1}^{*}(x(N-1)) = \min_{u(N-1)} [J(x(N-1), u(N-1))] \tag{8}$$

For step k $(0 \le k < N-1)$, the cost-to-go function is

$$J_{k}^{*}(x(k)) = \min_{u(k)} [J(x(k), u(k)) + J_{k+1}^{*}(x(k+1))] \tag{9}$$

where $J_{k}^{*}(x(k))$ is the optimal cost-to-go function at state $x(k)$ from step k to the end of the driving cycle. $J(x(k), u(k))$ is the instantaneous cost at step k. $x(k+1)$ is the state in step $(k+1)$ after the control $u(k)$ is executed at step k.

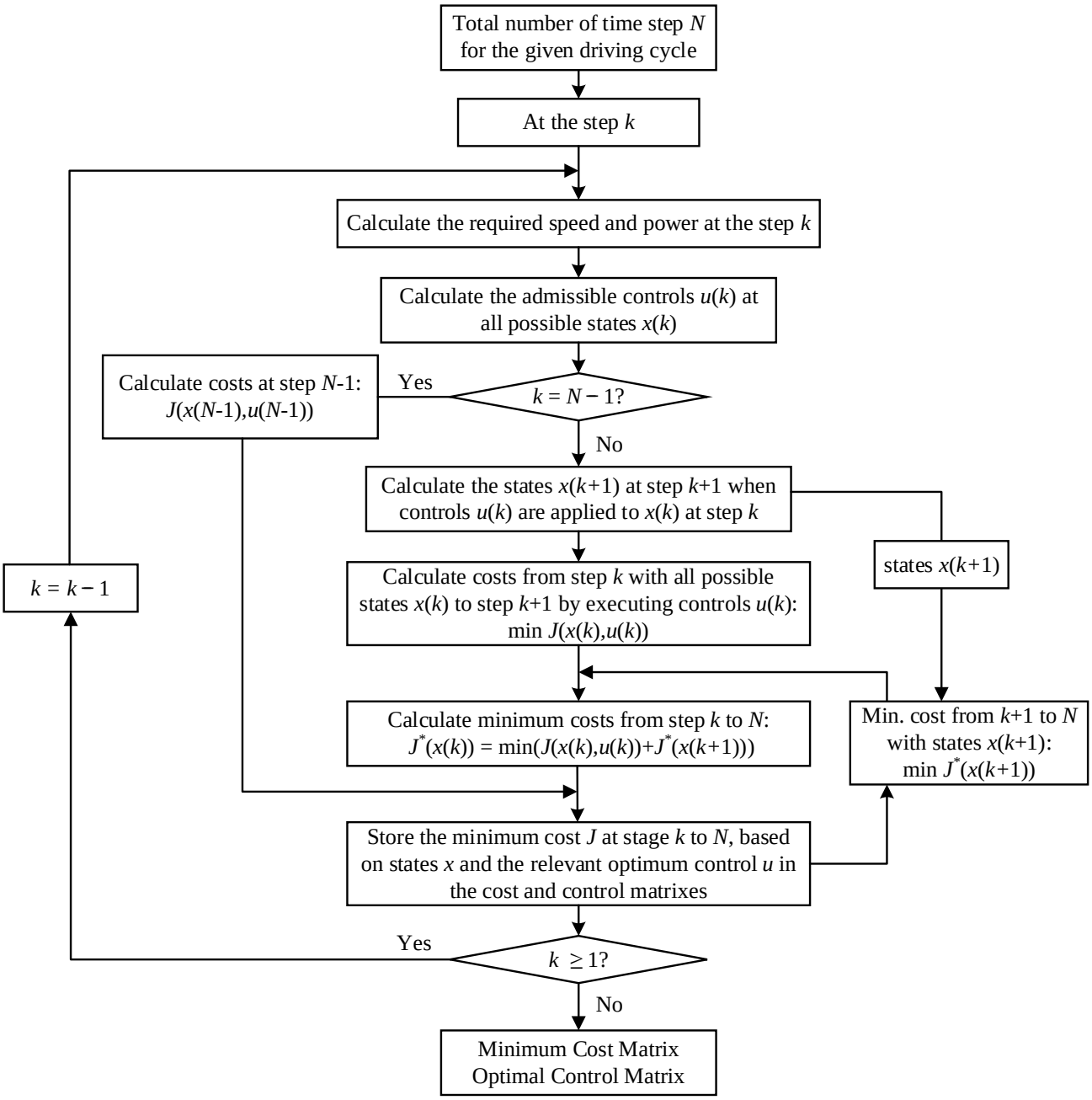

Fig. 3. Flow chart of DP solving procedure

Regarding the EF optimization over driving cycles in this research, the EF and battery SOC are the control and state variables, respectively. Both of them are discretized into finite grids before DP problem is formulated. In DP optimization process, all feasible control grids at every state will be found at each time step of the given driving cycle, subject to the constraints imposed in Eq. (11). The corresponding instantaneous cost can be evaluated by Eq. (10), following by searching the minimum cumulative cost from the current step to the last step by Eq. (15). By proceeding backward from the terminal of the driving cycle, the optimal EF trajectory can be achieved. The flow

chart of DP solving procedure is presented in Fig. 4, where the cost at each step is the equivalent fuel consumption, the required vehicle speed is given by the selected driving cycle, and the power demand is calculated by Eq. (4).

B. Driving Cycle Selection and Construction for DP Optimization

In general, a well-trained neural network has superior performance in the classification and prediction arena within the data range being utilized during the training phase [25]. Thus, the driving cycles selected for training dataset generation should correctly represent the diversity of the real-world driving conditions, this is, preferably include different driving patterns as much as possible to promote the generalization of neural networks. Besides, a sufficient number of data samples is required to guarantee the training effect of the neural network. Given the concerns mentioned above, five representative driving cycles, recommended by Liu et al. [26], are selected to generate the training dataset, which are NEDC, HWFET, UDDS, LA92 and US06. In Liu's study, 23 standard driving cycles were classified into five categories by using clustering analysis methods. The selected five driving cycles are the representatives of each driving cycle category. Moreover, WLTC and a real-world customized cycle, namely CQ1, are also included in the training data. WLTC is a prevalent standard driving cycle, frequently introduced to design and evaluate powertrain-related techniques, such as EMS [27] and thermal management systems [28]. CQ1, shown in Fig. 5, is tested in Chongqing and provided by the industrial partner.

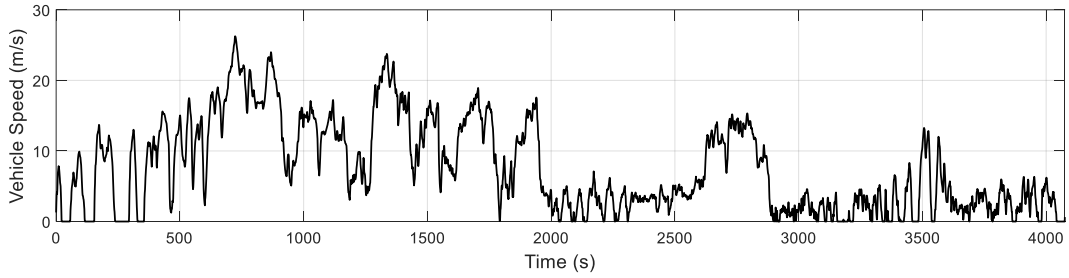

Fig. 4. Speed profile of CQ1 driving cycle

Due to the specifications of the selected PHEV in this research, the specified standard and real-world driving cycles have to be repeated several times to fully deplete the battery energy. Otherwise, the simple charge-depletion mode should be selected as EMS, as the pre-stored electric energy is sufficient to drive the vehicle to reach the destination. More importantly, the length of the driving cycles must dramatically exceed the all-electric range (AER), to clearly demonstrate the benefits of the proposed EMS. Thus, in this research, the aforementioned driving cycles will be extended by repeating themselves until the cumulative propulsion energy demand exceeds twice upon the

maximum storable battery energy. For simplicity, the constructed driving cycle is named the original driving cycle followed by the number of replications. For example, NEDC_3 implies that the constructed driving cycle is composed of 3 repeated NEDC. The descriptions of all selected driving cycles are presented in Table II.

Table II. Constructed driving cycle descriptions

Driving Cycle	Description	Number of Replications
NEDC	New European Driving Cycle (NEDC) represents the typical usage of a car in Europe, consisting of 4 repeated urban driving cycle and 1 extra-urban driving cycle.	7
HWFET	Highway Fuel Economy Test (HWFET) represents smooth highway driving conditions.	5
UDDS	Urban Dynamometer Driving Schedule (UDDS) represents city driving conditions.	7
LA92	LA92 is designed to simulate realistic urban and suburban driving with more aggressive accelerations and more transients.	4
US06	US06 reflects the aggressive driving behaviors such as hard accelerations and decelerations coupled with high-speed driving.	5
WLTC	Worldwide harmonized Light vehicles Test Cycles (WLTC) includes urban, suburban, rural and highway driving scenarios, which has an equal division between urban and non-urban paths.	3
CQ1	Chongqing1 is the real-world driving cycle tested in Chongqing, China, including city and highway driving scenarios.	3

C. Training Dataset Processing and Analysis

1). Optimal Solution Analysis and Re-construction

The initial training dataset composes of the DP optimization results over all constructed driving cycles. Note that the deceleration segments of the driving cycle should be excluded in the training dataset, as the vehicle braking force controller is independent of the proposed ECMS. However, the power for electric accessories and road loads, such as rolling and air resistances, are still existed during the vehicle deceleration. Thus, when the vehicle deceleration rate is relatively low, the positive propulsion power is still required to satisfy the aforementioned power demand. In this driving scenario, the proposed ECMS is still expected to manage the energy flow distribution. As a result, the driving conditions with the negative power demand are omitted from the optimization results in advance of constructing the training dataset.

According to the concept of the ECMS, a low EF implies that electrical energy is cheaper than using fuel and, therefore, the controller encourages the use of battery energy. Conversely, a high EF implies that using electrical energy is expensive, thereby reducing battery usage or charging the battery. Thus, for a given driving condition, there exists a threshold for the EF that determines whether the engine is engaged to provide the propulsion power. Provided that the EF drops below the threshold, the engine will be turned off regardless of the specific EF value. On the contrary, the EF will significantly affect the power split between the engine and traction motors when the EF is above the threshold. In conclusion, when the engine is required to provide propulsion power to achieve minimum equivalent fuel consumption, the precision of the EF prediction is of considerable importance in realizing the optimal power distribution.

However, the summary of the DP optimization results, listed in Table III, shows that the engine-on factor, representing the percentage of time with operating the engine, is lower than 30% in cases of 4 constructed driving cycles including NEDC_7, USSD_7, LA92_4, and CQ1_3. It implies that the initial training dataset is biased towards the driving conditions without operating the engine, which potentially causes that the trained NN predicts the EF more accurately at engine-off scenario than that at engine-on. Given the importance of the EF prediction accuracy at engine-on scenario, the training dataset ideally should have an equal division between engine-on and engine-off scenarios. Thus, for each constructed driving cycle, the DP optimization results at engine-on scenario are constantly repeated until the engine-on factor is over 50%. The corresponding replications of engine-on duration are presented in Table III.

As a consequence of the proposed replication, the total samples of each re-constructed driving cycle are widely dispersed within the range of 1990 to 8768, as shown in ‘Re-constructed Results’ column in Table III. Hence, the re-constructed driving cycles should be repeated further to equalize the contribution of each case to the training dataset. The resulting total samples of the repeated re-constructed results are all around 8500, and the resulting replications for each case are listed in the last column of Table III.

Table III. Summary of DP 0ptimization result modification for NN training

Cases	Total Duration (s)	DP Optimization Results			Re-constructed Results			Replications of Re-constructed Results
		Engine-on Duration (s)	Engine-on Factor (%)	Total Samples	Replications of Engine-on Duration	Engine-on Factor (%)	Total Samples	
NEDC_7	8260	1076	21.7%	4963	4	52.5%	8191	1
HWFET_5	3825	1511	45.5%	3320	2	62.6%	4831	2
UDDS_7	7420	1210	23.6%	5138	4	55.2%	8768	1
LA92_4	5740	828	27.8%	2980	3	53.6%	4636	2
US06_5	2980	1207	60.7%	1990	1	60.7%	1990	4
WLTC_3	5400	1045	32.8%	3183	3	59.5%	5273	2
CQ1_3	4075	1006	20.6%	4887	4	50.9%	7905	1

2). Driving Feature Selection for NN Inputs

The input selection for both EF prediction NN and engine status classification NN is inspired by researches in using NN to recognize driving patterns [1, 29], generate SOC reference [20, 30], and predict EF [3, 31]. All candidates for NN inputs, 14 representative driving features in total, are summarized in Table IV.

Table IV. Driving feature candidates for NN inputs

In the past 120 seconds		Instantaneous Value
Average Speed	Average Deceleration	Battery SOC
Maximum Speed	Maximum Deceleration	Speed
Average Acceleration	Acceleration Time Ratio (accelerating time/total time)	Power Demand
Maximum Acceleration	Deceleration Time Ratio (decelerating time/total time)	Ratio of Distance Travelled to Total Distance
Idle Time Factor (idle time/total time)	Constant Speed Time Ratio (contend speed time/total time)	–

Hasan [32] claims that redundant input variables usually result in low generalization capabilities and, therefore, poor test performance. Accordingly, the dimension of the input layer should be appropriately reduced by eliminating the least effective and correlated features, while still sufficient enough to describe the underlying characteristics of the problem and small enough to generalize for other datasets [33]. In this research, PCA is utilized to reduce the number of driving features collected in the past 120 seconds. PCA is a popular statistical procedure that can reduce the dimensionality of the dataset while preserving as much of the data variation as possible [34]. As a result, the

PCA shows that the first three principal components account for around 82% of the observed variance of the driving features collected in the past 120 seconds.

To sum up, seven variables are imposed as the inputs of two NNs, which are the first three principal components of the driving features collected in the past 120 seconds, battery SOC, vehicle speed, power demand, and ratio of distance travelled to total distance.

D. EF Correction Module

In Xi's research [35], NN was utilized to predict the extender output power for the extended range electric vehicle (EREV). The proposed NN was well trained against the DP optimization results over three artificial driving cycles constructed by repeating US06 two, three, and six times, respectively. The NEDC was employed to construct 80-km, 120-km and 165-km simulation driving cycles, which were adopted to validate the trained NN controller performance. The simulation results evidenced that the proposed NN-based EMS has unacceptable adaptiveness to the trip length. To be specific, the battery SOC can amount to the desired SOC of 0.3 at the end of the trip only when the trip length is 120 km. For the case with a shorter trip length, the terminal SOC is around 0.5. On the contrary, the test vehicle operates in a charge-sustaining mode after arriving at 120-km mark, as the battery SOC has already reached the lower limit. Thus, Xi at el. [35] proposed introducing the electricity consumption per unit distance calculation module, Cor_P, to correct the predicted extender power output to ensure the terminal SOC of 0.3. Cor_P is defined as the ratio between the available battery capacity and the remaining range.

$$Cor_P = SOC_{rem} / D_{rem} = (SOC(t) - SOC_{terminal}) / (D_{total} - D(t)) \quad (10)$$

where SOC_{rem} is the available battery capacity. D_{rem} is the remaining distance from the current location to the end of the trip. $SOC(t)$ is the current battery SOC. $SOC_{terminal}$ is the desired terminal SOC. $D(t)$ and D_{total} is the travelled and total distance, respectively.

In this research, an aforementioned correction method is improved by nondimensionalizing the electricity consumption per unit distance, called SOC-distance factor. The nondimensionalization makes SOC-distance factor varying around a unit. Consequently, the correction can be directly and easily applied to the EF. The SOC-distance factor is expressed as,

$$\theta = \frac{(SOC(t) - SOC_{terminal})/(SOC_{max} - SOC_{terminal})}{(D_{total} - D(t))/D_{total}} \tag{11}$$

where SOC_{max} is the prescribed maximum SOC of 0.8 and $SOC_{terminal}$ is fixed as 0.29.

By implementing the EF correction, the optimal EF derived from the DP optimization will be divided by the proposed SOC-distance factor, which is regarded as the output dataset for the BRNN training. When the BRNN is implemented online as the EF predictor, the output predicted by the BRNN will be multiplied by the SOC-distance factor to achieve the inverse transformation. Note that the SOC-distance in the training dataset is calculated based on the optimization results, while that in online implementation is determined by the actual SOC and travelled distance at each instant. In this manner, the remaining distance of the trip proactively impacts the EF regulation and still reserves the optimality delivered by the DP optimization.

E. BRNN for EF Prediction

A multilayered neural network is adopted to predict EF dynamically, as illustrated in Fig. 6. The node number of the input layer is fixed as the length of the inputs. Three hidden layers are constructed with 15, 40 and 15 neurons in sequence. The single output node represents the EF in ECMS.

The Bayesian regularization algorithm is adopted to train the NN. Bayesian regularization is a mathematical process that converts a nonlinear regression into a "well-posed" statistical problem in the manner of a ridge regression [36]. During the training process, the number of nontrivial weights in NN, referred to as effective network parameters, is evaluated. Consequently, irrelevant neurons can be effectively deactivated. In this manner, the total number of weights is considerably smaller than that in a standard fully connected backpropagation NN. The resulting benefit is to reduce the potential of overfitting and overtraining, thereby improving the generalization ability of the neural network.

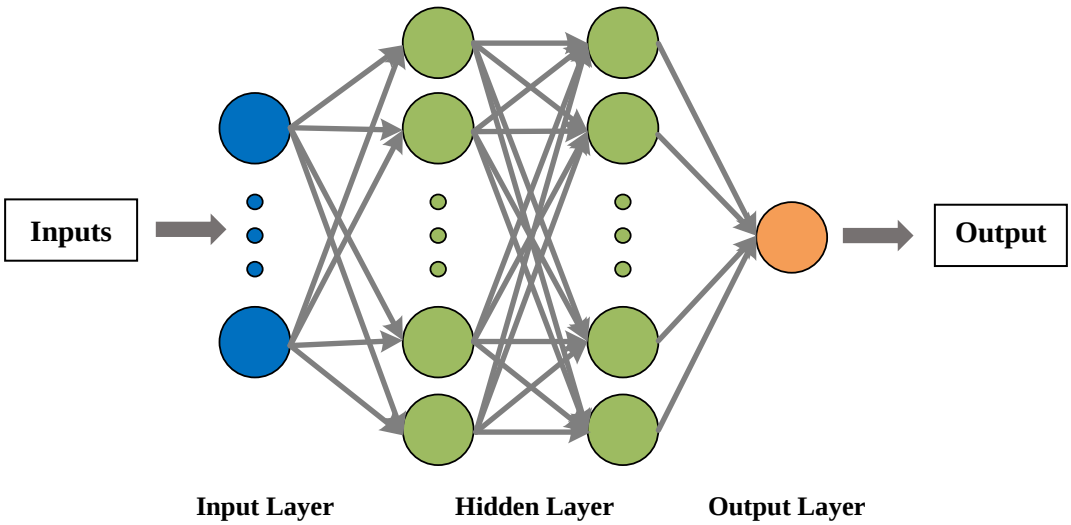

Fig. 5. Structure of EF BRNN predictor

Thus, the essence of the Bayesian Regularization algorithm is the transition from searching the minimum of the mean square error to minimize the following function [37],

$$M = \alpha E_W + \beta E_D \tag{12}$$

where α and β are hyperparameters. E_W is the sum of squares of the network weights. E_D is the sum of squared estimation errors, expressed as,

$$E_D = \frac{1}{2}\sum_{k=1}^{N} X_i(output(k) - target(k))^2 \tag{13}$$

where $output(k)$ is the NN output and $target(k)$ are the target data.

F. Classification NN Structure for Engine Status Prediction

Regarding EMS design, backpropagation NNs are extensively employed to identify the labeled features of the problem, due to its high-level classification accuracy and the ease of online implement. In this research, a backpropagation NN is developed to predict the engine status. When the engine status is predicted as shutdown, a reduction coefficient 0f 0.95 is applied to the predicted EF to ensure the engine shutdown event is consolidated. The input layer of the backpropagation NN is identical to that of the EF BRNN predictor. Four hidden layers are constructed with 8, 15, 15 and 2 neurons in sequence. The two outputs are two different engine statuses: engine-off and engine-on.

G. Quality Assessment of NN models

In advance of assessing the performance of two NNs, it is worth mentioning that the entire optimized dataset is randomly partitioned into training, validation, and testing in ratio of 70:15:15 for both EF BRNN predictor and engine status NN classifier. The training set is used to fit the NN to learn underlying patterns present in the given dataset. The validation set is used to provide an unbiased evaluation of the NN fitted by the training set while further tuning NN hyperparameters. The testing set is excluded during the training process and only utilized to assess the performance of the trained NN after the completion of the training and validation processes.

To have a clear perspective of NNs' performance, the confusion matrix for engine status classification and the regression plot for EF prediction are shown in Fig. 7 and Fig. 8, respectively.

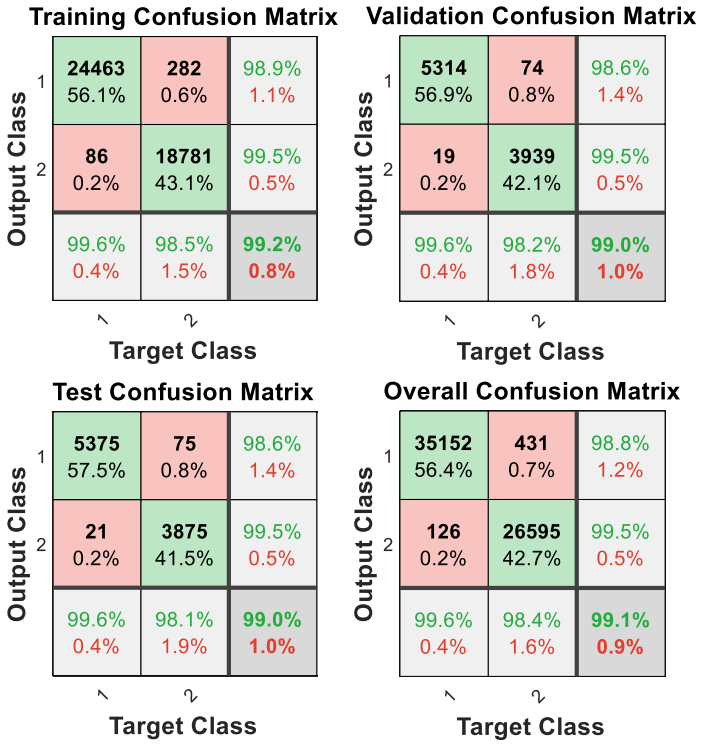

Fig. 6. Confusion matrix showing results of engine status classification

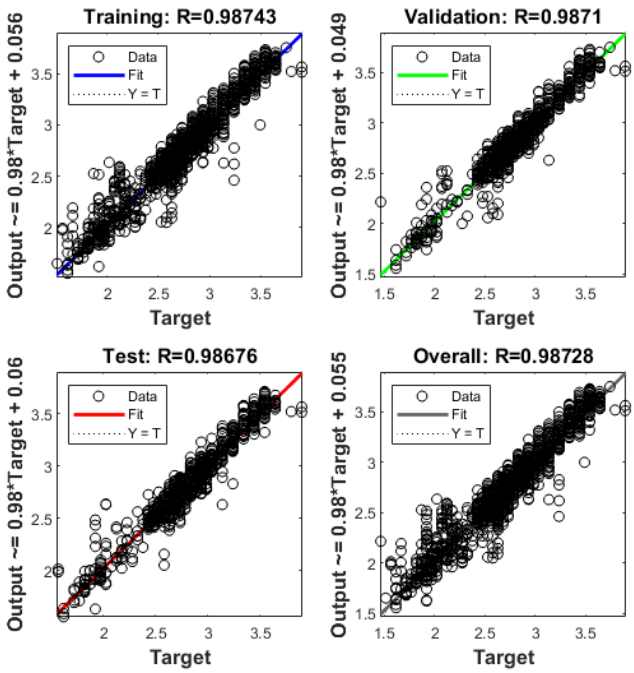

Fig. 7. EF regression plot comparing the target versus predicted values

In the confusion matrix, the green diagonal cells imply the number and percentage of correct detection cases, while the red cells correspond to misclassified observations. The bottom row summarizes the classification accuracy with respect to the target value, and the right-most column shows the classification accuracy with respect to the predicted labels. The total percentage of correct and incorrect detection cases are listed in the bottom-right cell highlighted in blue and red, respectively. In Fig. 7, category 1 indicates that the engine operates to provide the propulsion power or charge the battery, which category 2 is the engine-off. It is evident that the overall detection accuracy for engine status is 99.1% over a total of 62304 sampling points. The total percentage of misclassification cases for the engine-off is 0.7%, which is higher than that for the engine-on. It indicates that the trained engine status classifier is slightly biased towards the prediction of the engine-on. However, high overall detection accuracy validates the effectiveness of the online implementation of the trained engine status NN classifier.

The regression plots, shown in Fig. 8, present the BRNN outputs with respect to targets for training, validation, test, and combining all. It can be observed that the correlation between the predicted outputs and targets is reasonably strong over all data sets, with the regression coefficient (R) above 0.986. The closeness of the regression coefficient to 1 is an indication that the NN model fits the data well with a highly accurate prediction. Moreover,

the training stage has the highest regression coefficient of 0.98743. In terms of the validation and testing data sets, the overall patterns of the data points distribution are similar and a decreasing trend of the regression coefficient can be observed, which indicates that there is no overfitting in the EF NN predictor.

IV. NN-BASED ECMS VALIDATION AND TEST

In this section, all simulations are conducted based on the selected vehicle model with fixed component size in Section II, to validate and test the proposed NN-based ECMS. The driving cycles employed for the NN training are considered as the validating driving conditions, details of which are presented in Table II. While, two new driving cycles, WVUSUB and a real-world customized cycle CQ2, are defined as the testing driving profiles to verify the effectiveness of the proposed method. Similar to CQ1 driving cycle, CQ2 cycle is tested in Chongqing and the corresponding speed profile is shown in Fig. 9. Besides, the performance of the proposed method is analyzed through the comparison with DP optimization algorithm and an adaptive ECMS proposed by Xie [38]. The adaptive ECMS, regarded as the baseline controller for the validation, utilizes a proportional integral (PI) controller to adjust the EF, to ensure that SOC tracks the reference trajectory. A liner function of the remaining trip distance is considered as the expression of SOC reference trajectory. Additionally, all simulations were performed in Matlab environment on a laptop computer with a 3.1-GHz CPU and 8-GB memory.

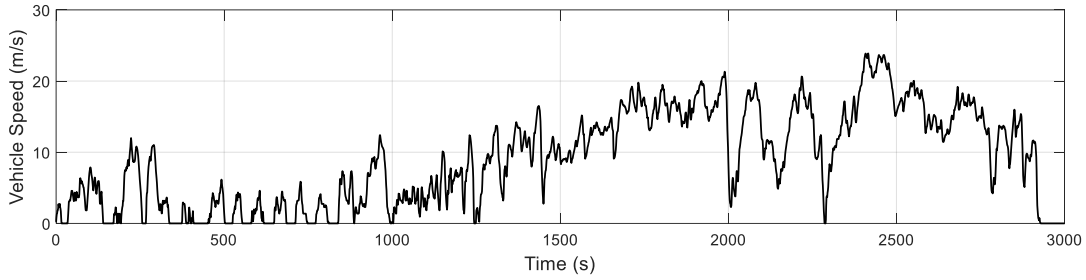

Fig. 8. Speed profile of CQ2 driving cycle

A. Performance Validation

The simulation results in terms of fuel economy over the validating driving cycles are listed in Table V. It can be seen that the PI-based ECMS always leads to the highest fuel consumption with the smallest computation time. NN-based ECMS can contribute to approximate 3 to 8 percentages less fuel consumption than that of the PI-based ECMS. Compared to the DP optimization method, NN-based ECMS is able to deliver similar percentages of fuel saving rate over all validating driving cycles. Up to 98.22% fuel saving of DP can be realized by the proposed

method under LA92_4 cycle, while the lowest is 95.35% fuel saving of DP under US06_5. On average, the proposed method can conduce to 96.81% fuel saving of DP over all validating driving cycles. Given the nearly identical terminal SOC for all test cases, it can be assumed that the fuel saving is merely attributed to the optimality of the controller itself. Thus, the near-optimal performance of the proposed method indicates that the EF BRNN predictor is well trained to predict the EF close to the optimal value and the proposed NN-based ECMS can approximate the optimal control actions. Besides, DP is the most time-consuming in all cases. Whereas, the proposed NN-based ECMS can significantly reduce the computation burden, which ensure the development of the real-time EMS.

Table V. Fuel consumption comparison over validating driving cycles

Cases	Control Strategy	Fuel Consumption (L)	Saving Rate (%)	Terminal SOC	Computation Time (s)
NEDC_7	PI-based ECMS	2.228	-	0.305	59.2
	NN-based ECMS	2.125	4.57 (97.34%)	0.303	181.0
	DP	2.070	7.05	0.290	1723.8
HWFET_5	PI-based ECMS	2.757	-	0.303	35.5
	NN-based ECMS	2.635	4.41 (96.26%)	0.303	74.6
	DP	2.540	7.87	0.291	784.5
UDDS_7	PI-based ECMS	2.269	-	0.292	44.5
	NN-based ECMS	2.158	4.88 (98.06%)	0.292	182.7
	DP	2.117	6.68	0.291	1920.3
LA92_4	PI-based ECMS	2.139	-	0.305	38.3
	NN-based ECMS	2.012	5.96 (98.23%)	0.293	114.0
	DP	1.977	7.58	0.291	1142.8
US06_5	PI-based ECMS	3.088	-	0.309	17.2
	NN-based ECMS	2.973	3.72 (95.35%)	0.302	57.7
	DP	2.841	7.99	0.291	602.8
WLTC_3	PI-based ECMS	2.366	-	0.299	31.9
	NN-based ECMS	2.290	3.22 (96.14%)	0.297	110.3
	DP	2.205	6.83	0.291	1098.3
CQ1_3	PI-based ECMS	2.550	-	0.290	66.9
	NN-based ECMS	2.456	3.67 (96.32%)	0.290	244.5
	DP	2.369	7.09	0.291	2386.5

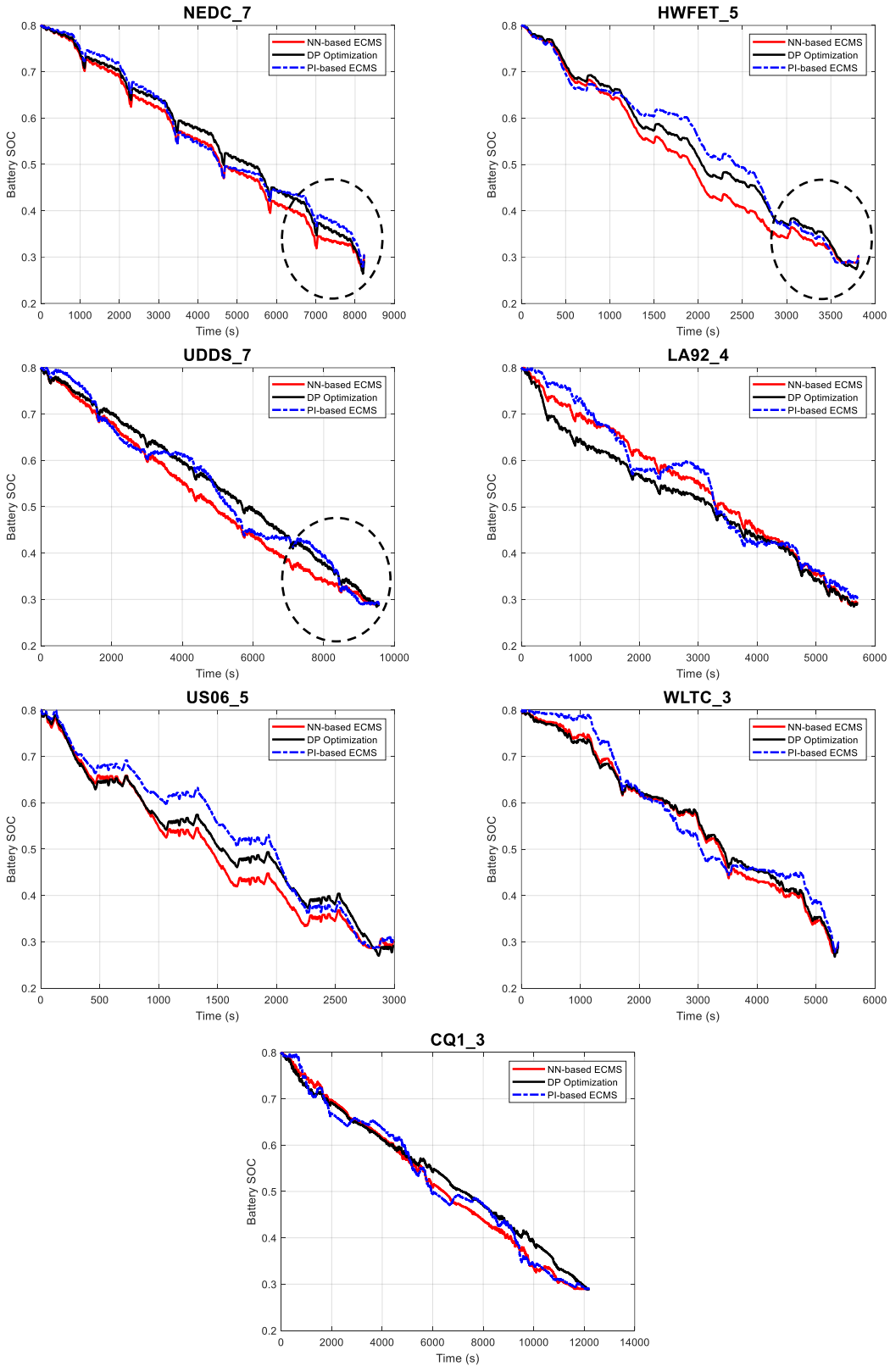

Fig. 9. SOC trajectories of different methods under training driving cycles

Although both the DP and proposed method can ensure that the terminal SOC reaches the prescribed value, the diversity of the SOC trajectory during the trip can contribute to completely different power distribution and, therefore, fuel consumption. Thus, the SOC trajectories of different control methods for all validating cases are presented in Fig. 10. Overall, the trend of battery SOC based on the proposed NN-based ECMS is basically consistent with the optimal SOC trajectory generated by DP optimization. In particular, the battery SOC trajectories under the DP and NN-based ECMS overlap considerably over WLTC_3 and CQ1_3. Although slightly larger discrepancies of battery SOC trajectories are observed over the rest of validating driving cycles, the proposed method still can track the SOC variation patterns derived from DP optimization results. Note that the fuel consumption delivered by NN-based ECMS over such driving cycles, shown in Table V, is fairly similar to that of DP optimization. Hence, from the perspective of fuel economy, the observed SOC discrepancies appear to be acceptable.

Additionally, as indicated in Fig.10, the terminal battery SOC based on the proposed method can always be guaranteed within an acceptable deviation from the prescribed value of 0.29. It is worth mentioning that the terminal SOC is satisfied without the support of the SOC reference trajectory. It implies that the proposed SOC-distance factor is capable of adaptively correcting the EF online based on the reaming trip distance, thereby suppressing the excessive over-discharge or over-charge of the battery before the end of the trip. Take the case of HWFET_5 as an example. The proposed method intends to utilize the electrical energy to propel the vehicle before around 2500 s, which leads to a larger decreasing slope of the SOC trajectory than that of DP algorithm. Thereafter, the SOC discrepancy gradually becomes smaller and two SOC trajectories almost completely overlap at around 3500 s. This SOC adjustment can be explained as follow. According to Eq. (17), for a given remaining trip distance the relatively low SOC will yield the decrease of the SOC-distance factor, thereby enlarging the EF predicted by the BRNN. As a consequence, the engine usage will be promoted to drive the vehicle or charge the battery and, therefore, prevent the over-discharge of the battery. As is illustrated in the highlighted regions in Fig. 10, the adaptive EF correction based on the battery SOC and remaining trip distance becomes more influential on the SOC adjustment when approaching the end of the trip.

Moreover, it can be found in Fig. 10 that SOC trajectories of DP method are below the prescribed SOC lower bound of 0.29 near the end of the trip in some cases. This is because that the deceleration at the end of the trip results in a battery charging event. Thus, the battery has to be deliberately depleted below the SOC lower bound before the deceleration, to ensure that the terminal SOC reaches the prescribed lower bound. Under NEDC_7, HWFET_5, US06_5, and WLTC_3, this phenomenon is evident due to the significant deceleration at the end of the trip. However, the over-discharge of battery is forbidden in the proposed NN-based ECMS. When the SOC attempt to drop below the lower bound, the energy control strategy will be switched from the proposed method to Charging-Depleting/Charge-Sustaining (CD/CS) to maintain the SOC above the limit.

B. Performance Assessment under Testing Driving Cycles

To further demonstrate the effectiveness of the proposed NN-based ECMS, two different driving cycles are introduced as the testing driving cycles, which are WVUSUB and CQ2. Note that the testing driving cycles are excluded in the driving conditions for NN training. Thus, the adaptiveness and optimality of the proposed method can be revealed by evaluating its control performance over the selected testing driving cycles. Similar to the validating driving cycles, the original WVUSUB and CQ2 cycles are repeated 7 and 3 times respectively, to ensure that the corresponding cumulative propulsion energy demand surpasses twice upon the maximum storable battery energy.

Table VI. Fuel consumption comparison over testing driving cycles

Cases	Control Strategy	Fuel Consumption (L)	Saving Rate (%)	Terminal SOC	Computation Time (s)
WVUSUB_7	PI-based ECMS	1.997	-	0.291	57.0
	NN-based ECMS	1.931	3.36 (95.96%)	0.291	254.2
	DP	1.856	7.07	0.291	2330.0
CQ2_3	PI-based ECMS	2.153	-	0.294	41.7
	NN-based ECMS	1.938	9.99 (98.69%)	0.293	193.0
	DP	1.913	11.15	0.292	1876.8

The fuel economy assessment over testing driving cycles is listed in Table VI. As can be found, the terminal SOC differences among all selected control strategies are insignificant in both two test cases. Thus, the presented remarkable fuel saving rates demonstrate the outstanding energy management performance of DP algorithm and the proposed NN-based ECMS. Furthermore, the proposed method is able to realize 95.96% and 98.69% fuel savings of DP in WVUSUB_7 and CQ2_3, respectively. These results corroborate that the optimal information

learned from the training driving cycles can contribute to attaining the near-optimal control actions for the other cycles, thanks to the distinguished generalization of BRNN. Moreover, compared with DP method, the significant reduction of computation time can be found by implementing the proposed NN-based ECMS. It indicates that the proposed method is more preferable in real-time applications.

The comparison of engine operating points between DP and NN-ECMS, shown in the normalized engine map in Fig. 11, can further verify the optimality of the proposed method, as there is an obvious overlap of operating point distribution between two strategies in both WVUSUB_7 and CQ2_3 cases. For further performance comparison, the SOC trajectories are shown in Fig. 12 for WVUSUB_7 and CQ2_3, respectively. As is illustrated in Fig. 12, DP and NN-based ECMS induce a reasonably similar trend of the SOC trajectory. Under WVUSUB_7 cycle, the proposed method slightly prioritizes the usage of the electric power rather than the engine, which results in lower SOC comparing to that of DP. However, due to the employment of the EF correction in the proposed method, the excessive SOC reduction stimulates the preservation of electrical energy, especially when approaching the end of the trip. As a result, the SOC based on the proposed method successfully reaches the expected terminal SOC of 0.29. On the contrary, the engine is marginally over-used before halfway into CQ2_3 cycle, yielding a higher SOC than that of DP. Thereafter, the EF correction module effectively inhibits the engine operation and, therefore, gradually reduce the SOC close to the optimal SOC trajectory.

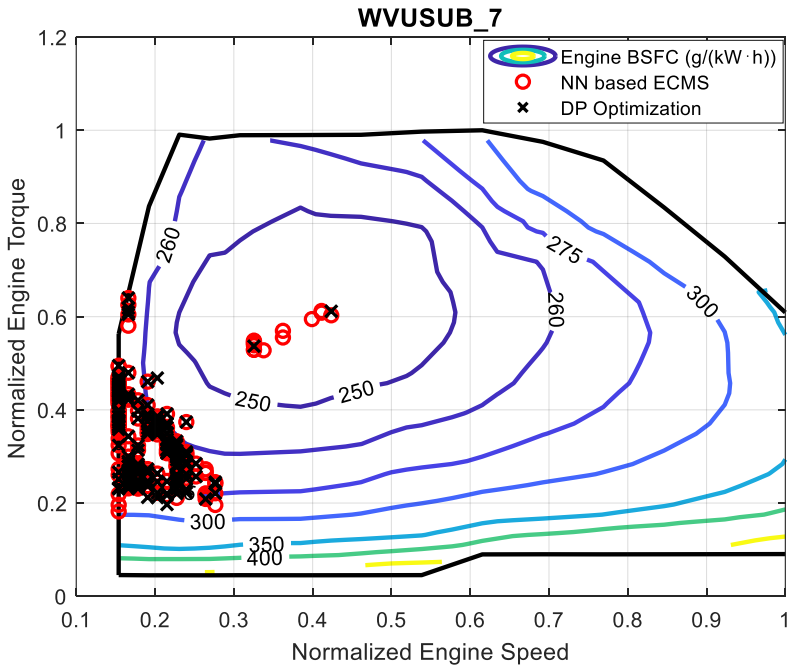

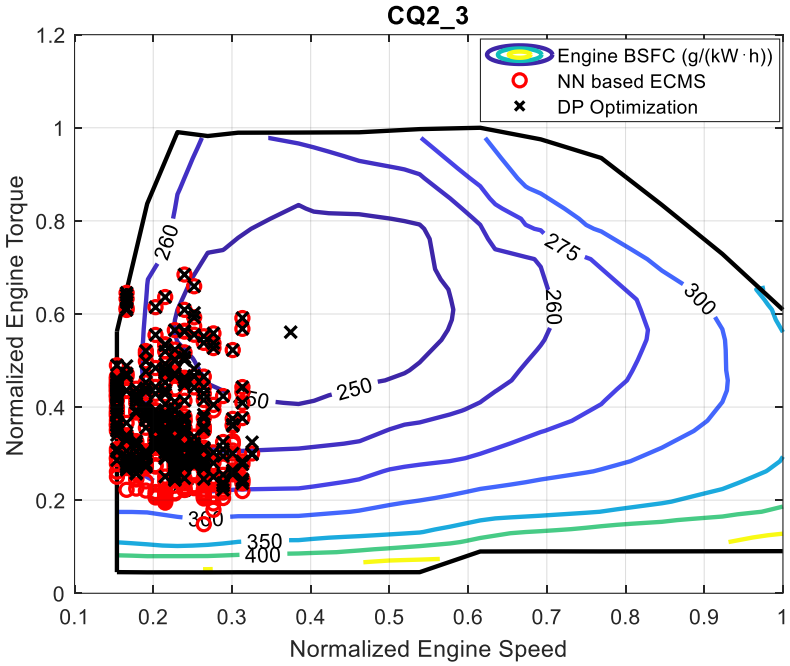

Fig. 10. Comparison of the distribution of engine working points under the two testing driving conditions

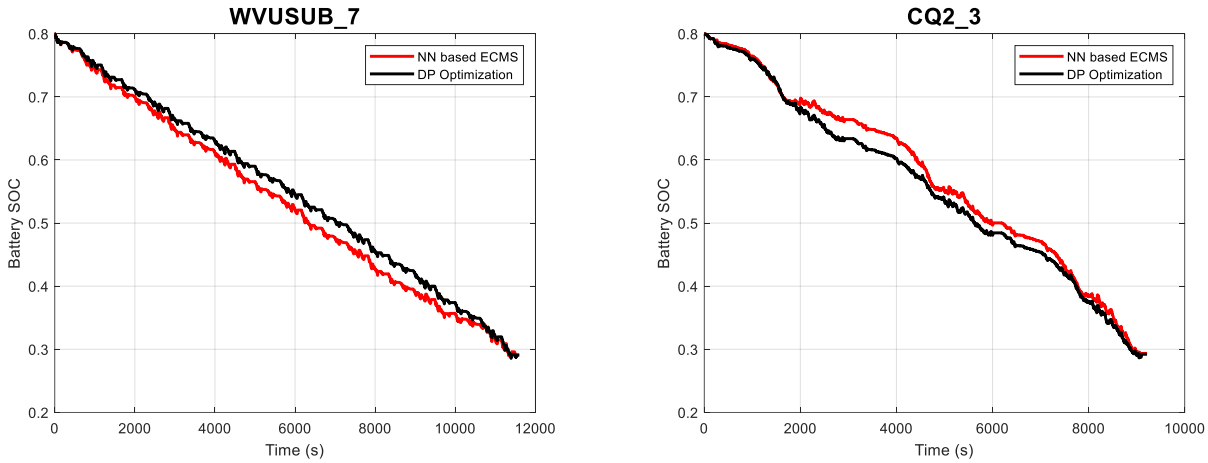

Fig. 11. SOC trajectory comparison under WVUSUB_7 (right) and CQ2_3 (left)

V. CONCLUSION

In this study, an NN-based ECMS is developed for PHEVs. The proposed energy management strategy contains two NNs. The BRNN, a well-known data-driven method due to its excellent generalization ability, is embedded to dynamically identify the near-optimal EF for the ECMS. Additionally, a backpropagation NN is employed to predict the engine on/off, aiming to eliminate the side effect of the EF prediction error. The corresponding adjustment mechanism is to recognize the optimal engine status based on the global optimal

information learned from the training stage. Then, a downscaling factor will be applied to the predicted EF when the backpropagation NN suggests deprioritizing the engine operating. As a result, the lower value of EF can consolidate the engine shutdown event and prevent sub-optimal power distribution within the powertrain system. The NN quality assessment shows that, by taking advantage of the global optimality of DP, the trained backpropagation NN can achieve an exceptional detection accuracy of up to 99.1%, while the BRNN obtains the regression coefficient of 0.98743 between NN outputs and targets. The outstanding NN quality can enhance the overall performance of the proposed method, thereby realizing the near-optimal power distribution.

The other novelty of the proposed method is the EF correction method. Given that there is no SOC reference generation in the proposed method, the terminal SOC has to be constrained strictly by an alternative method. Thus, the SOC-distance factor, which is a function of the remaining travel distance and the instantaneous available battery capacity, is deployed to scale the EF online. Based on the definition of SOC-distance factor, the over-discharge of the battery conduces to the increase of SOC-distance factor and, therefore, reduces the value of the EF to promote the use of the engine. Note that the optimal EF derived from the DP optimization will be divided by the corresponding SOC-distance factor calculating based on the optimal results. Afterward, the processed EF is regarded as the outputs in the training data for the EF BRNN predictor. Regarding online implementation, the output predicted by the BRNN will be multiplied by the SOC-distance factor which is determined by the remaining trip distance and the current available battery SOC. In this manner, the remaining distance of the trip proactively impacts the EF regulation and still reserves the optimality delivered by the DP optimization.

The control performance validation and testing disclose that the proposed NN-based ECMS induces comparable fuel economy to DP optimal solution. Under all validating driving cycles, the proposed method attains an average 96.82% fuel saving of global optimization results. Regarding the driving cycles unexposed to the NN training, 95.96% and 98.69% fuel saving of DP optimization are expected by the proposed method under WVUSUB_7 and CQ2_3, respectively. The promising simulation results verify the effectiveness and adaptiveness of the NN-based ECMS.

Next step work will focus on further performance improvement of the proposed NN-based ECMS by considering additional influential factors, such as the driving patterns and the future traffic condition. Although

aforementioned influential factors have been investigated and implemented in EMSs [39-42], less effort has been made to investigate the effects of these factors on the NN-based ECMS. Furthermore, all validation and testing cases are conducted only with the initial SOC of 0.8 in this research. In the future, the adaptiveness of the NN-based ECMS to various initial SOCs will be developed. Besides, driving cycles employed in this research are customized to remarkably exceed AER to demonstrate the advantage of the proposed method. However, an AER estimation is required in practice to determine whether the proposed EMS or the charge-depletion mode is activated. Therefore, the AER estimation method will be investigated in the future research.

ACKNOWLEDGEMENTS

The work presented in this paper is funded by the National Natural Science Foundation (No. 52002046) in part, the Chongqing Fundamental Research and Frontier Exploration Project (No. CSTC2019JCYJ-MSXMX0642) in part, the Science and Technology Research Program of Chongqing Municipal Education Commission (No. KJQN201901539) in part, and the EU-funded Marie Skłodowska-Curie Individual Fellowships Project under Grant 845102-HOEMEV-H2020-MSCA-IF-2018 in part. Any opinions expressed in this paper are solely those of the authors and do not represent those of the sponsors.

REFERENCES

1. Lin, X., et al., *Optimal adaptation equivalent factor of energy management strategy for plug-in CVT HEV*. Proceedings of the Institution of Mechanical Engineers, Part D: Journal of Automobile Engineering, 2018. **233**(4): p. 877-889.
2. Hu, X., Y. Zou, and Y. Yang, *Greener plug-in hybrid electric vehicles incorporating renewable energy and rapid system optimization.* Energy, 2016. **111**: p. 971-980.
3. Xie, S., et al., *An artificial neural network-enhanced energy management strategy for plug-in hybrid electric vehicles.* Energy, 2018. **163**: p. 837-848.
4. Yang, C., et al., *Robust coordinated control for hybrid electric bus with single-shaft parallel hybrid powertrain.* IET Control Theory & Applications, 2014. **9**(2): p. 270-282.
5. Wang, S., et al., *Fuzzy Adaptive-Equivalent Consumption Minimization Strategy for a Parallel Hybrid Electric Vehicle.* IEEE Access, 2019. **7**: p. 133290-133303.
6. Zhang, Y., et al., *Energy management strategy for plug-in hybrid electric vehicle integrated with vehicle-environment cooperation control.* Energy, 2020: p. 117192.
7. Zhang, F., et al., *Energy Management Strategies for Hybrid Electric Vehicles: Review, Classification, Comparison, and Outlook.* Energies, 2020. **13**(13).
8. Marano, V., et al., *Comparative study of different control strategies for plug-in hybrid electric vehicles*. 2009, SAE Technical Paper.
9. Tran, D.D., et al., *Thorough state-of-the-art analysis of electric and hybrid vehicle powertrains: Topologies and integrated energy management strategies.* Renewable and Sustainable Energy Reviews, 2020. **119**.

10. Huang, Z. and Y. Wang, *Optimization-Based Energy Management Strategy for a 48-V Mild Parallel Hybrid Electric Power System.* Journal of Energy Resources Technology, 2020. **142**(5).
11. Kommuri, N.K., et al., *Evaluation of a Modified Equivalent Fuel-Consumption Minimization Strategy Considering Engine Start Frequency and Battery Parameters for a Plugin Hybrid Two-Wheeler.* Energies, 2020. **13**(12).
12. Paganelli, G., *Design and control of a parallel hybrid car with electric and thermal powertrain*. 1999, University of Valenciennes.
13. Tian, X., et al., *An adaptive ECMS with driving style recognition for energy optimization of parallel hybrid electric buses.* Energy, 2019. **189**.
14. Tulpule, P., et al. *Optimality assessment of equivalent consumption minimization strategy for PHEV applications*. in *Dynamic Systems and Control Conference*. 2009.
15. He, Y., et al., *An energy optimization strategy for power-split drivetrain plug-in hybrid electric vehicles.* Transportation Research Part C: Emerging Technologies, 2012. **22**: p. 29-41.
16. Zhang, C., et al. *Role of trip information preview in fuel economy of plug-in hybrid vehicles*. in *Dynamic Systems and Control Conference*. 2009.
17. Tian, H., et al., *Adaptive Fuzzy Logic Energy Management Strategy Based on Reasonable SOC Reference Curve for Online Control of Plug-in Hybrid Electric City Bus.* IEEE Transactions on Intelligent Transportation Systems, 2018. **19**(5): p. 1607-1617.
18. Feng, T., et al., *A Supervisory Control Strategy for Plug-In Hybrid Electric Vehicles Based on Energy Demand Prediction and Route Preview.* IEEE Transactions on Vehicular Technology, 2015. **64**(5): p. 1691-1700.
19. Han, L., X. Jiao, and Z. Zhang, *Recurrent Neural Network-Based Adaptive Energy Management Control Strategy of Plug-In Hybrid Electric Vehicles Considering Battery Aging.* Energies, 2020. **13**(1).
20. Montazeri-Gh, M. and Z. Pourbafarani, *Near-Optimal SOC Trajectory for Traffic-Based Adaptive PHEV Control Strategy*. IEEE Transactions on Vehicular Technology, 2017. **66**(11): p. 9753-9760.
21. Torreglosa, J.P., et al., *Analyzing the Improvements of Energy Management Systems for Hybrid Electric Vehicles Using a Systematic Literature Review: How Far Are These Controls from Rule-Based Controls Used in Commercial Vehicles?* Applied Sciences, 2020. **10**(23): p. 8744.
22. Sivertsson, M. and L. Eriksson, *Design and Evaluation of Energy Management using Map-Based ECMS for the PHEV Benchmark.* Oil & Gas Science and Technology – Revue d'IFP Energies nouvelles, 2014. **70**(1): p. 195-211.
23. Burden, F. and D. Winkler, *Bayesian regularization of neural networks.* Artificial neural networks, 2008: p. 23-42.
24. Bellman, R.E. and S.E. Dreyfus, *Applied dynamic programming*. 2015: Princeton university press.
25. Thirumalainambi, R. and J. Bardina. *Training data requirement for a neural network to predict aerodynamic coefficients*. in *Independent Component Analyses, Wavelets, and Neural Networks*. 2003. International Society for Optics and Photonics.
26. Liu, Y., et al., *Energy Management Strategy Optimization of HEV based on Driving Pattern Recognition.* Journal of Mechanical Transmission, 2016. **05**: p. 64-69.
27. Nguyen, B.-H., et al., *Real-time energy management of battery/supercapacitor electric vehicles based on an adaptation of Pontryagin's minimum principle.* IEEE transactions on Vehicular Technology, 2018. **68**(1): p. 203-212.
28. Xu, J., et al., *Modelling and control of vehicle integrated thermal management system of PEM fuel cell vehicle.* Energy, 2020: p. 117495.
29. Li, H., et al., *Real-Time Control Strategy for CVT-Based Hybrid Electric Vehicles Considering Drivability Constraints.* Applied Sciences, 2019. **9**(10).
30. Han, L., X. Jiao, and Z. Zhang, *Recurrent neural network-based adaptive energy management control strategy of plug-in hybrid electric vehicles considering battery aging.* Energies, 2020. **13**(1): p. 202.
31. Tian, X., et al., *An ANFIS-based ECMS for energy optimization of parallel hybrid electric bus.* IEEE Transactions on Vehicular Technology, 2019. **69**(2): p. 1473-1483.
32. Sildir, H., E. Aydin, and T. Kavzoglu, *Design of feedforward neural networks in the classification of hyperspectral imagery using superstructural optimization.* Remote Sensing, 2020. **12**(6): p. 956.

33. Kavzoglu, T. and P. Mather, *The use of backpropagating artificial neural networks in land cover classification.* International journal of remote sensing, 2003. **24**(23): p. 4907-4938.
34. Syms, C., *Principal components analysis*. 2008, Elsevier.
35. Xi, L., et al., *Intelligent energy management control for extended range electric vehicles based on dynamic programming and neural network.* Energies, 2017. **10**(11): p. 1871.
36. Burden, F. and D. Winkler, *Bayesian regularization of neural networks*, in *Artificial neural networks*. 2008, Springer. p. 23-42.
37. Okut, H., *Bayesian regularized neural networks for small n big p data.* Artificial neural networks-models applications 2016.
38. Xie, S., et al., *A Pontryagin Minimum Principle-Based Adaptive Equivalent Consumption Minimum Strategy for a Plug-in Hybrid Electric Bus on a Fixed Route.* Energies, 2017. **10**(9).
39. Montazeri-Gh, M. and M. Mahmoodi-K, *Optimized predictive energy management of plug-in hybrid electric vehicle based on traffic condition.* Journal of cleaner production, 2016. **139**: p. 935-948.
40. Montazeri-Gh, M. and A. Fotouhi, *Traffic condition recognition using the k-means clustering method.* Scientia Iranica, 2011. **18**(4): p. 930-937.
41. Watanabe, T. and S. Katsura. *On-line recognition of driving road condition using support vector machine*. in *2011 IEEE International Conference on Industrial Technology*. 2011. IEEE.
42. Zeng, Y., J. Sheng, and M. Li, *Adaptive real-time energy management strategy for plug-in hybrid electric vehicle based on Simplified-ECMS and a novel driving pattern recognition method.* Mathematical Problems in Engineering, 2018. **2018**.